Journal of Nuclear Materials 442 (2013) S869–S872

Contents lists available at SciVerse ScienceDirect

Journal of Nuclear Materials

journal homepage: www.elsevier.com/locate/jnucmat

On determination of the constitutive behavior of tempered martensitic steels from micro-indentations: Application to Eurofer97 steel

P. Spätig *, N. Ilchuk

Fusion Technology-Materials, CRPP EPFL, Association EURATOM-Confédération Suisse, 5232 Villigen PSI, Switzerland

ARTICLE INFO

Article history:
Available online 11 January 2013

ABSTRACT

This paper proposes a simple but powerful approach to determine the constitutive equation of tempered martensitic steels from micro-hardness tests. Finite element simulations were used to investigate the plastic flow in the contact region between the tip and the specimen. The simulations were validated by experimental tests carried out on the tempered martensitic steel Eurofer97 using a simple constitutive Ludwik-type equation. A series of simulations using different constitutive behaviors representative of possible irradiation-induced changes were run. In all cases, a pile-up of material against the indenter tip was observed that is strongly dependent on the constitutive law. Considering the real contact height of the indenter with the material, it was shown that the hardness scales with an averaged value of the flow stress over 30% of plastic strain. In addition, the parameters of Ludwik equation were shown to be determinable from the two experimental quantities that are the hardness and the ratio between the contact height and the penetration depth of the tip.

1. Introduction

Among the small specimen test techniques used to determine mechanical properties, micro-hardness and nano-hardness experiments have been extensively used to extract parameters of the plastic flow [1,2]. Hardness measurement requires a very small amount of material, which makes it an attractive method to follow the evolution of mechanical properties with irradiation, providing that a reliable method exists to correlate hardness data to other standard data. However, hardness is not a fundamental property of materials, so relating hardness to the flow stress (taken at a given strain or averaged over a strain range) is not straightforward [3]. Based upon both theoretical and experimental considerations, various analytical expressions between hardness and yield stress or ultimate tensile strength have been proposed [4–6]. These empirical calibrations are not universal in the sense that the parameters of the expressions are material dependent. Therefore, there is no guarantee that a calibration well-established for an unirradiated material remains the same for the same material after irradiation. A close look at the residual profile of the indentation and analysis of this pile-up with finite element simulations yields additional useful information on the strain-hardening of the materials as it was demonstrated in Santos et al. [7]. When hardness experiments are performed on materials that develop a pile-up or sink-in, the hardness, defined by the load divided by the projected contact area, can be determined from the experimental load-penetration depth curves only if one correctly accounts for the pile-up or sink-in geometry. Indeed, the contact height between the indenter tip and the materials is a function of the pile-up or sink-in geometry, which in turn depends on the overall constitutive behavior. Therefore, the hardness can be properly calculated only if a reliable model is available to relate the penetration depth to the contact height. This study was undertaken to search for an appropriate description of the contact area during the indent experiment on tempered martensitic steel. Using the knowledge of the experimental values of hardness and pile-up geometry, a simple method is proposed to determine the true-stress–strain curve.

2. Materials, indentations, and finite element models

The material used in this research is reduced activation Eurofer97 steel, heat E83697, 25-mm-thick plate, produced by Böhler AG. The chemical composition (wt.%) is Fe–8.9Cr–0.12C–0.46Mn–1.07W–0.2V–0.15Ta. The heat-treatment was at 1253 K for 0.5 h and tempering at 1033 K for 1.5 h. This steel is fully martensitic after quenching.

The microhardness tests were performed with an instrumented G200 MTS nanoindenter equipped with a high load module that allows reaching a maximum load of 10 N. A Vickers tip was used.

Indentations were simulated with ABAQUS 6.10-3 code [8]. The code calculates the deformed configurations based on the J_2 plastic flow theory and associated flow rule. Two finite element models were built: one with a four-sided pyramid having the Vickers tip

* Corresponding author. Address: CRPP/EPFL, ODGA-C102A, 5232 Villigen PSI, Switzerland. Tel.: +41 56 310 29 34; fax: +41 56 310 45 29.
E-mail address: philippe.spatig@psi.ch (P. Spätig).

0022-3115/$ - see front matter © 2013 Elsevier B.V. All rights reserved.
http://dx.doi.org/10.1016/j.jnucmat.2013.01.003

geometry and one with an axisymmetric rigid cone tip. The axisymmetric indenter tip with a vertical angle $\phi = 70.3°$ was designed to yield the same projected area-to-depth ratio as that of the Vickers tip. Among the output of the calculations, the load-penetration depth, the profile of the specimen surface, and the indenter-specimen contact height were required.

Taking advantage of the Vickers tip geometry, only a quarter of the specimen-tip assembly was considered (see Fig. 1). The quarter specimen has the following dimensions: $400 \times 400 \times 400$ μm (width × length × height). It was meshed with 140,000 elements of the type 8-node linear brick, reduced integration. The size of the elements is biased to have a very fine mesh below the indenter tip to catch the strong stress/strain gradient occurring under the tip. The tip itself was meshed with 9638 elements of the type 4-node tetrahedron. The contact between the tip and the specimen was assumed frictionless. The diamond tip deforms elastically and the following values of the Young's modulus and Poisson's ratio were used: $E = 1141$ GPa and $\nu = 0.07$.

The axisymmetric model was actually developed to save computing time while remaining representative of the Vickers model, at least qualitatively, which is why the projected area-to-depth ratio is identical to that of the Vickers. The geometry of the model is shown in Fig. 2. In this case, the cone is considered as a fully rigid body. The dimensions of the specimens are also $400 \times 400 \times 400$ μm (width × length × height). The mesh is refined under the tip. For this model, only 10,000 elements of the type 4-node axisymmetric quadrilateral, reduced integration were employed.

To determine the dependence of the tip-specimen contact area on the material constitutive behavior, we used an expression of the Ludwik equation type for the true-stress–strain curves as:

$$\sigma = \sigma_y + A\varepsilon_p^{0.5} \tag{1}$$

where σ_y is the yield stress, and A is the strain-hardening coefficient. A fit to experimental true stress–strain data of Eurofer97 at room temperature yields $\sigma = 530 + 680\ \varepsilon_p^{0.5}$, which was found to be satisfactory. It should be mentioned that a physically based constitutive law that is more accurate but more complicated was proposed by Spätig et al. [9]. However, for this parametric study, the Ludwik's power law is sufficient. As stated in the Introduction, one of the main goals of this study is to calculate the actual projected contact area for various constitutive behaviors representative of tempered martensitic steel in the unirradiated and irradiated conditions, for irradiations performed in the hardening temperature regime (<723 K). Since this regime is characterized by an increase of the yield stress with a concomitant decrease of the strain-hardening capacity, σ_y was varied from 530 to 800 MPa and the strain-hardening coefficient A was decreased down to 50 while the strain-hardening exponent n remained at 0.5. In total, 14 different constitutive behaviors were used in this work. The parameters of Eq. (1) are

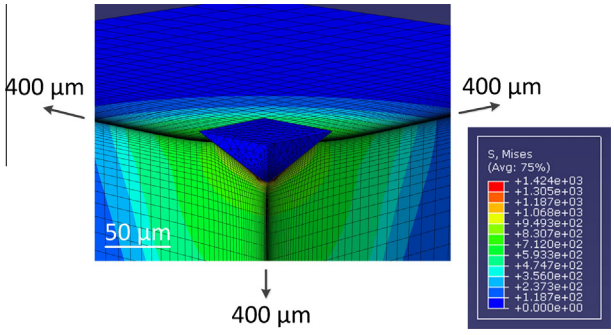

Fig. 1. Sketch of the 3D Vickers tip – specimen model.

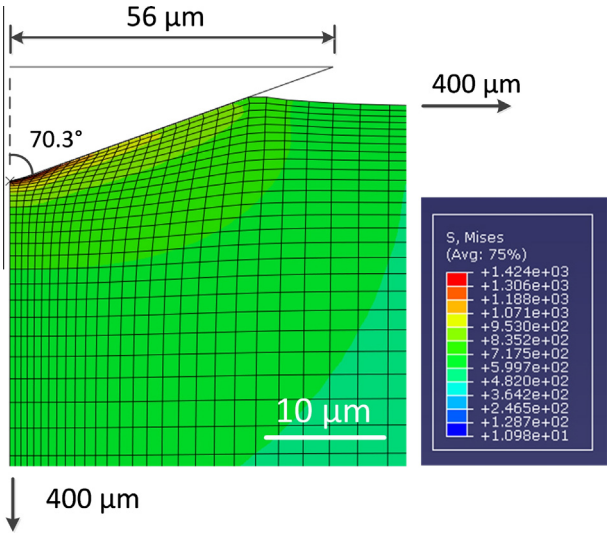

Fig. 2. Sketch of the axisymmetric cone tip – specimen model.

Table 1
Parameters of the different constitutive behaviors used for the finite element simulations.

σ_y (MPa)	A (MPa)	n	α defined as $h_c = \alpha * h_p$
530	680	0.5	1.1016
530	390	0.5	1.139
530	100	0.5	1.1964
530	50	0.5	1.206
630	680	0.5	1.1011
630	390	0.5	1.138
630	100	0.5	1.1877
630	50	0.5	1.97
730	680	0.5	1.0985
730	390	0.5	1.132
730	100	0.5	1.1774
730	50	0.5	1.194
800	100	0.5	1.169
800	50	0.5	1.181

summarized in Table 1. For the sake of clarity, only three curves are plotted in Fig. 3, corresponding to $\sigma_y = 530$ MPa, $A = 680$; $\sigma_y = 530$ MPa, $A = 100$; and $\sigma_y = 800$ MPa, $A = 50$ MPa to illustrate the difference in the strain-hardening capacity and in the yield stress we considered. The elastic properties of the specimens were given by: $E = 210$ GPa and $\nu = 0.3$.

To validate the three-dimensional (3D) model of the Vickers indenter and to compare it with the experimental load-penetration depth of the micro-hardness experiment, simulations for the 3D and axisymmetric model were run using the actual measured experimental true-stress–strain curve.

3. Results and discussion

First, the experimental load-penetration depth of the Vickers indentation is presented along with the calculated curves of the 3D finite element model in Fig. 4. As can be seen, a very good correspondence between the two curves was found, in particular for the loading part. Fig. 4 also shows the calculated curve for the axisymmetric model that appears to be very close to the 3D Vickers one despite the difference in the tip geometry. Owing to this fact, the axisymmetric model was regarded as being a very good approximation of the Vickers to realize this parametric study. The hardness values from the simulations were calculated using the applied load divided by the projected contact area at the result-

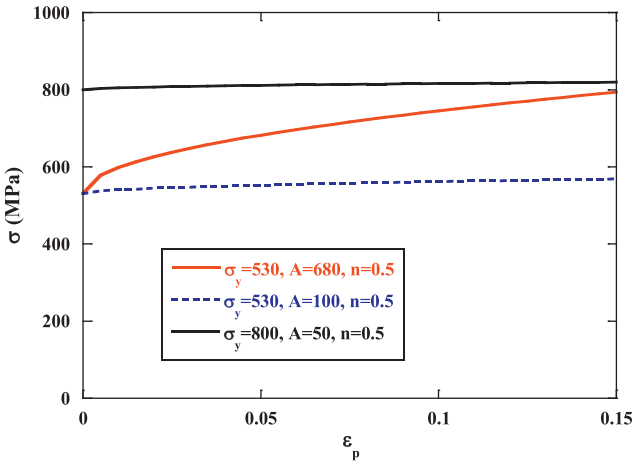

Fig. 3. Example of true-stress–strain curves used as input for the FE simulations.

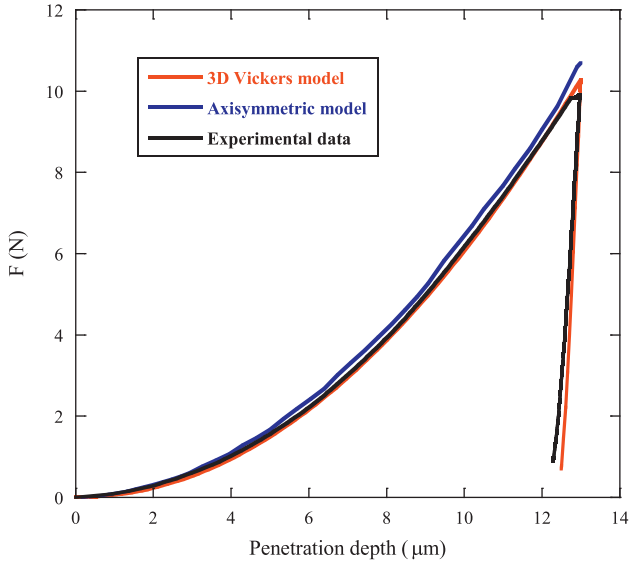

Fig. 4. Comparison between the Vickers indentation experimental curve, the 3D, and the axisymmetric simulation.

ing penetration depth of 13 μm. The hardness is equal to 1907 and 2011 MPa for the 3D and axisymmetric model, respectively; these values are consistent with those obtained from the real test and determined according the standard procedure (load/projected contact area) and being equal to 2150 MPa.

The specimen surface profile analysis during the simulation shows that a pile-up of material exists in the contact area between the tip and the specimen. We emphasize here that such a behavior deviates significantly from the standard method described by Oliver and Pharr [10] where the contact area is deduced from a model that assumes material sink-in only instead of a pile-up characterizing the tip-specimen contact region and which is used currently as a default hardness calculation algorithm for the most instrumented nano-indenters. However, the influence of the pile-up on the hardness was already studied by finite element simulations by Bolshakov and Pharr on materials different from steels [11]. In the case of pile-up, the tip-specimen contact height is evidently greater than the penetration depth, while the opposite is true for the sink-in. To determine the hardness correctly, one has to establish a correlation between the contact height (h_c) and the penetration depth (h_p). Plotting the h_c against h_p for all the simulations shows that a simple linear relationship holds between these two quantities. The correlation is shown in Fig. 5 for the 3D Vickers model. In this

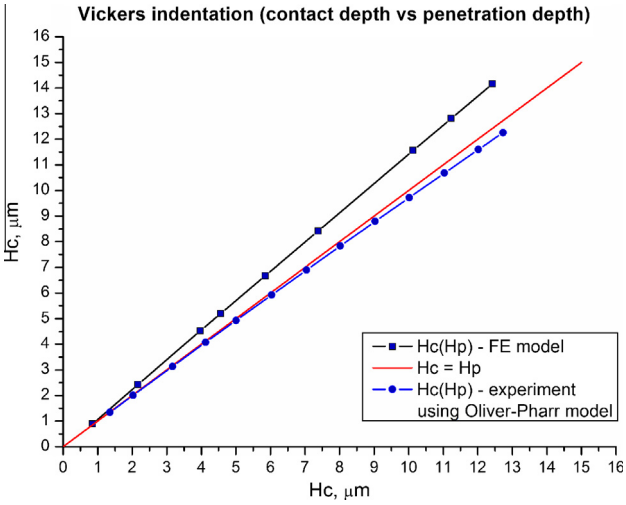

Fig. 5. Contact height h_c versus penetration depth hp for the 3D Vickers model.

figure, the real contact height dependence on penetration depth obtained from simulations is compared to the contact height dependence on penetration depth calculated according to Oliver–Pharr model using experimental data showing the linear increase of the difference between both.

In order to quantify the effect of the constitutive behavior on the height of the pile-up, we define a coefficient α as:

$$\alpha = \alpha[\sigma(\varepsilon_p)] = \frac{h_c[\sigma(\varepsilon_p)]}{h_p} \tag{2}$$

The coefficient α is obtained for the different constitutive behaviors indicated in Table 1.

The results of the simulations with the axisymmetric models allow insight into the dependence of the constitutive behavior on hardness and on α. The simulations were run with the power laws given in Table 1 and to a penetration depth of 13 μm, which corresponds to the range of loads from 9.2 to 13.4 N. The contact height and the reaction force on the indenter were extracted at 13 μm penetration depth and the corresponding hardness was calculated from these parameters. Significantly different hardness values were found. Using the work of He et al. [12], a calibration between hardness and an averaged value of flow stress $\langle\sigma_{\text{flow}}\rangle$ can be determined. This is a natural approach recognizing that the hardness curve shape is mediated by both the elastic and plastic properties from the very beginning of the deformation. However, the plastic strain range over which the flow stress has to be averaged is not known *a priori*. Thus, to determine the averaging plastic strain range of the flow stress, the hardness data of all simulations were plotted against $\langle\sigma_{\text{flow}}\rangle$ and the linear correlation coefficient R was calculated as a function of the plastic strain considered. The best coefficient R was obtained for $\langle\sigma_{\text{flow}}\rangle$ averaged over 30% of true strain. The corresponding value is presented in Fig. 6. This finding is somewhat different from that of He et al. [12] who proposed a calibration between hardness and $\langle\sigma_{\text{flow}}\rangle$ averaged over 10% only. The reason of this apparent disagreement is likely to lie in the analytical description of the constitutive behavior. Indeed, He et al. employed a true-stress–strain curve that saturates at large strain while the power law used in this study does not saturate. This observation is important as it shows that one has to know the constitutive behavior of the material over a rather large strain range to gain confidence in any calibration between hardness and $\langle\sigma_{\text{flow}}\rangle$. This also demonstrates that a universal relationship for all classes of metals and alloys does not exist.

The effects of the constitutive behavior on the relation $h_c(h_p)$ are illustrated in Fig. 7 where the α coefficient is plotted against the

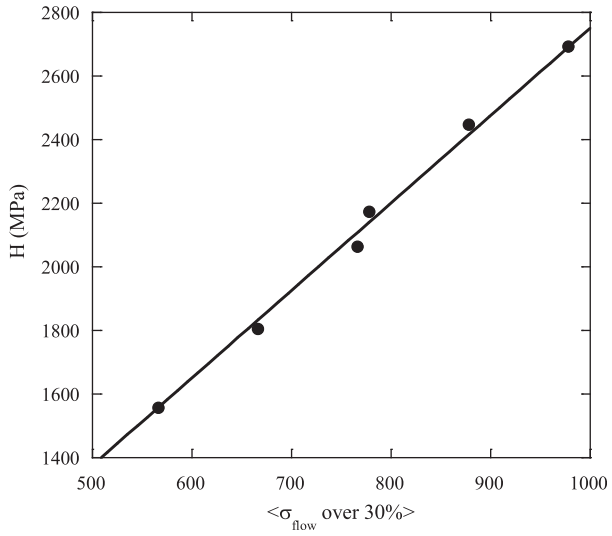

Fig. 6. Hardness versus $\langle\sigma_{flow}\rangle$ averaged over 30%.

hardness. Clearly, the height of the pile-up is not a simple function of hardness (or of $\langle\sigma_{flow}\rangle$), but depends on the strain-hardening capacity and the yield stress. In Fig. 7, the data linked by the blue lines have the same strain-hardening coefficients (A and n) but different yield stresses, while those linked by the black lines correspond to identical yield stress but different strain-hardening coefficients. Decreasing both σ_y and the strain-hardening capacity promotes the formation of the pile-up but again knowing $\langle\sigma_{flow}\rangle$ or the hardness only is not sufficient to predict the height of the pile-up. The information in Fig. 7 is sufficient to determine the constitutive behavior. Indeed, both the height of the pile-up and the hardness can be determined experimentally, and from these two quantities (which actually correspond to the coordinates of a single point (H–α) in the plot), one can obtain the constitutive behavior as defined by Eq. (1). The approach uses only two parameters to describe the constitutive behavior: σ_y and A. In other words, the knowledge of the pair (H–α) defines the pair (σ_y–A). For practical purposes, a more precise determination of the pair (σ_y–A) from Fig. 7 can be obtained by drawing more lines separated by smaller increments $\Delta\sigma_y$ and ΔA than done in this study. In principle, the smaller the increments, the smaller the domains defined by the intersections of the lines, and the better the resolution. Finally,

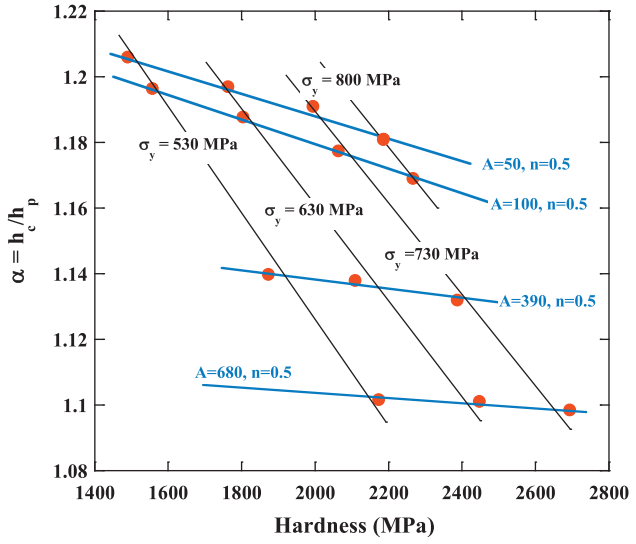

Fig. 7. α coefficient ($=h_c/hp$) versus hardness.

we also remind here that for the tempered martensitic steels in the unirradiated and irradiated condition the uniform elongation measured with tensile tests is usually much smaller than 30%, Thus the described procedure allows to assess the true-stress–strain curve beyond the necking onset, which is essentially a geometrical instability inherent of the tensile test.

4. Conclusions

Vickers micro-hardness test and finite element simulations were undertaken to determine the actual contact area of the indenter with the specimen as a function of the indenter penetration depth for tempered martensitic steels. Eurofer97 steel was used as the reference material to validate the finite element model. The Vickers indentations were carried out up to a load of 10 N with a fully instrumented G200 MTS nano-indenter. The experiments were supplemented with 3D finite element simulations that were in good agreement with the experimental load–displacement curve. Axisymmetric simulations using a conical indenter with the same area function as the Vickers were in good agreement with the Vickers 3D simulations in terms of load–displacement curve. Thus, the axisymmetric model was used to realize a parametric study to assess the effect of the yield stress and strain-hardening coefficient on the indenter-specimen contact area. The post-yield behavior was described by a simple power lower of the plastic strain. The yield stress and strain-hardening coefficients A were modified in a way representative of possible irradiation-induced change of the constitutive law, i.e., an increase of the yield stress and decrease of strain-hardening capacity. For tempered martensitic steels having a rather moderate strain-hardening capacity, the findings are:

(1) A pile-up of material forms against the indenter tip from the very beginning of the deformation. This phenomenon leads to a contact area that is at least 10% greater than that predicted by Oliver–Pharr model. Therefore, a correct determination of hardness on the tempered martensitic steel requires either experimental measurements of pile-up height following testing (to get a reasonable estimate of contact area) or finite element simulation modeling.
(2) When considering materials that obey a Ludwik-type constitutive law with an exponent equal to 0.5 then the hardness value scales with the flow stress averaged over 30% of plastic strain.
(3) The true-stress–strain curve of power law type with the exponent fixed at 0.5 can be precisely determined. A bi-univocal correspondence exists between the contact height and hardness with the yield stress and strain-hardening coefficient.

References

[1] Y.P. Sharkeev, S.A. Gashenko, O.V. Pashchenko, V.P. Krivobokov, Surf. Coat. Technol. 91 (1997) 20.
[2] C.-H. Hsu, J. Nucl. Mater. 518 (1986) 141–143.
[3] A. Mkaddem, F. Gassara, R. Hambli, J. Mater. Proc. Technol. 178 (2006) 111.
[4] C. Rubenstein, Trans. ASME 48 (1981) 786.
[5] G.R. Speich, H. Warlimont, J. Int. Steel Inst. 206 (1968) 385.
[6] J.R. Cahoon, Metall. Trans. 3 (1972) 3040.
[7] C. Santos, G.R. Odette, G.E. Lucas, T. Yamamoto, J. Nucl. Mater. 258–263 (1998) 452.
[8] ABAQUS Version 6.10-3, 3DS-Dassault Systèmes, 2011.
[9] P. Spätig, R. Bonadé, G.R. Odette, J.W. Rensman, N. Campitelli, P. Mueller, J. Nucl. Mater. 367–370 (2007) 527.
[10] W.C. Oliver, G.M. Pharr, J. Mater. Res. 19 (1) (2004) 3.
[11] A. Bolshakov, G.M. Pharr, J. Mater. Res. 13 (4) (1998) 1049.
[12] M.Y. He, G.R. Odette, T. Yamamoto, D. Klingensmith, J. Nucl. Mater. 367–370 (2007) 556.